Bistability of patterns of synchrony in Kuramoto oscillators with inertia

Igor V. Belykh,[1] Barrett N. Brister,[1] and Vladimir N. Belykh[2,3]
[1]*Department of Mathematics and Statistics and Neuroscience Institute, Georgia State University, 30 Pryor Street, Atlanta, Georgia 30303, USA*
[2]*Department of Control Theory, Lobachevsky State University of Nizhny Novgorod, 23, Gagarin Ave., 603950 Nizhny Novgorod, Russia*
[3]*Department of Mathematics, Volga State University of Water Transport, 5A, Nesterov Str., Nizhny Novgorod 603950, Russia*

(Received 3 April 2016; accepted 9 August 2016; published online 24 August 2016)

We study the co-existence of stable patterns of synchrony in two coupled populations of identical Kuramoto oscillators with inertia. The two populations have different sizes and can split into two clusters where the oscillators synchronize within a cluster while there is a phase shift between the dynamics of the two clusters. Due to the presence of inertia, which increases the dimensionality of the oscillator dynamics, this phase shift can oscillate, inducing a breathing cluster pattern. We derive analytical conditions for the co-existence of stable two-cluster patterns with constant and oscillating phase shifts. We demonstrate that the dynamics, that governs the bistability of the phase shifts, is described by a driven pendulum equation. We also discuss the implications of our stability results to the stability of chimeras. *Published by AIP Publishing.*
[http://dx.doi.org/10.1063/1.4961435]

Patterns of synchronized clusters are observed in many networks, ranging from neuronal populations to power grids. Despite significant interest among physicists and applied mathematicians, the emergence and hysteretic transitions between stable clusters in a network of identical oscillators have still not been fully understood. In particular, the celebrated Kuramoto model of identical phase oscillators is known to exhibit multiple spatio-temporal patterns, including co-existing clusters of synchrony and chimera states in which some oscillators form a synchronous cluster, while the others oscillate asynchronously. Rigorous analysis of the stability of clusters and chimeras in the finite-size Kuramoto model has proved to be challenging, and most existing results are numerical. In this paper, we contribute toward the rigorous understanding of the emergence of stable clusters in networks of identical Kuramoto oscillators with inertia. We derive the conditions under which two patterns of synchrony stably co-exist and demonstrate how inertia affects the hysteretic transitions between the patterns. Our stability results also shed light on the emergence of transient and stable chimeras.

I. INTRODUCTION

Pattern synchronization has been shown to be central for the functioning of a wide spectrum of biological and technological networks.[1–7] Two important cooperative rhythms of pattern dynamics are complete and cluster synchronization. Complete synchronization, in which all oscillators evolve in unison, and its dependence on network structure have received a great deal of attention in the literature.[8–12] Cluster synchronization is observed when the network splits into groups of coherent oscillators, but the dynamics between the groups is asynchronous.[13–23] The existence of clusters of perfect synchrony in networks of identical oscillators is strictly defined by intrinsic symmetries of the network.[18,19] These symmetries are defined as permutations of the nodes that preserve all internal dynamics and all couplings.[20] Permissible cluster partitions in a given complex network can be found via available combinatorial algorithms.[22,23] Central questions in the study of cluster synchronization are (i) under what conditions are the clusters stable? and (ii) do the clusters defined by perfect symmetries persist under parameter mismatch? These stability[13,15,16,21] and persistence[17] questions have been addressed for different classes of dynamical networks; yet, the full picture is far from being complete.

The classical Kuramoto model is a network of 1D phase oscillators with mean-field coupling.[24–26] The oscillators are assumed to be non-identical with different natural frequencies, whose distribution is defined by a given probability density function. The model has a coupling threshold such that the oscillators, evolving incoherently for a weak coupling, synchronize when the coupling exceeds the threshold. Transitions from the incoherent state to various forms of partial frequency synchronization, measured by an order parameter, have been studied in the Kuramoto model with different regular and random coupling configurations (see a review paper[27] for more details). Historically, the emergence of patterns of synchrony was studied in the Kuramoto model, under the assumption of an infinitely large network size, allowing for the mean field approximation. A breakthrough in the rigorous study of the infinite-dimensional Kuramoto model was made with the discovery of the Ott-Antonsen ansatz[29] which reduces the analysis of a restricted class of phase states to low dimensional dynamics.[28–30] Motivated by real-world finite-size networks, the interest has now shifted towards the analysis of finite-dimensional Kuramoto models.[31–35]

When oscillators in the classical Kuramoto model have identical frequencies, the network has no coupling threshold and complete synchronization is locally stable for any, arbitrarily weak coupling strength.[27] This had been the main obstacle in realizing that the identical oscillators can also exhibit complex patterns of synchrony whose emergence may be hidden by the stable synchronous state. This general perception of somewhat uninspiring dynamics of identical Kuramoto models has changed with the discovery of chimera states[36–39] in which structurally and dynamically identical oscillators spontaneously break into groups where some oscillators synchronize whereas the others remain incoherent. There is now a vast literature on the study of chimera states in the Kuramoto model as well as in other models of biological and mechanical systems (see an extensive review[39] for more details and references). Most studies of the stability of chimera states are numerical, with the exception of a few theoretical investigations, including the ones performed for large[40,41] and small networks[42,43] of 1D phase oscillators.

Inspired by the adaptive frequency model of firefly synchronization[44] where the oscillators are capable of adjusting their natural frequencies, the classical Kuramoto model of 1D phase oscillators was extended to a model of 2D oscillators with inertia.[45,46] This Kuramoto model with inertia was shown to exhibit various synchronization transitions[45–47] and hysteristic phenomena,[48] including intermittent chaotic chimeras[49] and reentrant synchronous regimes.[50] Existing analytical studies of the collective dynamics of the Kuramoto model with inertia mainly aim at (i) the stability of complete synchronization,[51–53] (ii) bifurcations leading to its loss,[54] and (iii) non-trivial phase transitions to synchrony in the presence of noise.[50]

In this paper, we go further to analyze the co-existence of stable patterns of synchrony in two symmetrically coupled populations of identical Kuramoto oscillators with inertia. We derive exact results on the stability of a two-cluster synchronous state in which the population splits into two clusters of synchronized oscillators, but there is no synchrony between the clusters. We reduce the system, governing the dynamics of the phase shift between the clusters, to the pendulum equation.[55] As a result, the phase shift between the clusters can remain constant or can periodically rotate its phase, depending on the choice of initial conditions. This yields the bistability of patterns of synchrony where a pattern with a constant inter-cluster phase shift stably co-exists with a breathing pattern when the inter-cluster phase shift evolves in time. Our stability analysis also addresses the emergence of transient and stable chimeras.

The layout of this paper is as follows. First, in Sec. II, we present and discuss the network model. In Sec. III, we study the existence of synchronous clusters and perform the analysis that allows for describing the dynamics of the synchronous clusters in terms of the limit sets of the pendulum equation. We derive the conditions on the bistability of synchronous dynamics which are explicit in the parameters of the network model. In Sec. IV, we analyze the variational equations for the stability of the synchronous cluster and obtain the main stability results of this paper. In Sec. V, we present a numerical example which supports our analytical results. Finally, Section VI contains concluding remarks.

II. TWO-GROUP NETWORK: IDENTICAL ROTATORS, DIFFERENT GROUP SIZES

Following previous studies in networks of Kuramoto models without[38,43] and with inertia,[49] we consider a two-group network of 2D rotators

$$\begin{aligned} m\ddot{\theta}_i+\dot{\theta}_i &= \omega+\frac{\mu}{N+M}\sum_{j=1}^{N}\sin\left(\theta_j-\theta_i-\alpha\right)\\ &\quad+\frac{\nu}{N+M}\sum_{j=1}^{M}\sin\left(\varphi_j-\theta_i-\alpha\right),\quad i=1,\ldots,N\\ m\ddot{\varphi}_k+\dot{\varphi}_k &= \omega+\frac{\mu}{N+M}\sum_{j=1}^{M}\sin\left(\varphi_j-\varphi_k-\alpha\right)\\ &\quad+\frac{\nu}{N+M}\sum_{j=1}^{N}\sin\left(\theta_j-\varphi_k-\alpha\right),\quad k=1,\ldots,M. \end{aligned} \tag{1}$$

Here, the network is divided into two groups of oscillators of sizes N and M, with all-to-all symmetrical coupling within and between the two groups, such that the intragroup coupling strength, μ, is stronger than the intergroup coupling strength, ν. Variables θ_i and φ_k represent the phases of oscillators in the first and second groups, respectively. The oscillators are assumed to be identical, with identical frequency ω, phase lag $\alpha\in[0,\pi/2)$ and inertia m. The model (1) is an extension of the Abrams *et al*. chimera model,[38,43] consisting of two groups of 1D phase oscillators with Kuramoto-Sakaguchi coupling.[24,56] In the model (1), we use the 2D Kuramoto oscillator with inertia as the individual cell model and consider non-equal group sizes. These two properties will allow for deriving analytical conditions on the stability of clusters of synchrony, exhibiting two types of co-existing behavior where (i) the phase between the synchronized clusters remains fixed and (ii) the phase between the clusters oscillates.

By rescaling time $\tau=\mu t/(N+M)$ and parameter $\beta=\mu m/(N+M)$, and using a rotating frame of reference $\Theta_i=\theta_i-\omega t+c$, $\Phi_k=\varphi_k-\omega t+c$, where c is a constant, we can cast the model (1) into a more compact form

$$\begin{aligned} \beta\ddot{\Theta}_i+\dot{\Theta}_i &= \sum_{j=1}^{N}\sin\left(\Theta_j-\Theta_i-\alpha\right)\\ &\quad+\gamma\sum_{j=1}^{M}\sin\left(\Phi_j-\Theta_i-\alpha\right),\quad i=1,\ldots,N\\ \beta\ddot{\Phi}_k+\dot{\Phi}_k &= \sum_{j=1}^{M}\sin\left(\Phi_j-\Phi_k-\alpha\right)\\ &\quad+\gamma\sum_{j=1}^{N}\sin\left(\Theta_j-\Phi_k-\alpha\right),\quad k=1,\ldots,M, \end{aligned} \tag{2}$$

where $\gamma=\nu/\mu$ represents the ratio between the intra- and intergroup couplings such that $\gamma\in(0,1)$.

III. EXISTENCE OF SYNCHRONOUS CLUSTERS

A. Cluster partition

The connectivity matrix G of network (2) has a block structure

$$G = \begin{pmatrix} J_{N,N} & \gamma J_{N,M} \\ \gamma J_{M,N} & J_{M,M} \end{pmatrix}, \tag{3}$$

where $J_{N,N}$, $J_{M,M}$, $J_{N,M}$, and $J_{M,N}$ are $N \times N$, $M \times M$, $N \times M$, and $M \times N$ all-ones matrices, respectively.

In general, clusters of perfect synchrony are determined by a network decomposition into the disjoint subsets of oscillators $V = V_1 \cup \ldots \cup V_d$, $V_p \cap V_q = \varnothing$ defined by the equalities of the oscillator states. If this cluster decomposition is flow-invariant with respect to the vector field of the network system, then the corresponding manifold $D(d)$ is invariant and defines d synchronous clusters. Synchronous clusters exist if the graph vertices have a corresponding balanced coloring.[18–20] Every cluster corresponds to a coloring in which two oscillators have the same color if and only if their states are completely synchronized. Oscillators colored in this way create a coloring map. A coloring of the vertices is balanced, if each oscillator of color i has the same number of inputs from the oscillators of color j, for all i and j. A minimal balanced coloring is a balanced coloring with the minimal number of colors.

In the context of the network (2), a necessary condition for oscillators to form a cluster is the equal row sum constraint. In fact, the first N rows of matrix G, corresponding to the first group of oscillators, have row sums equal to $N + \gamma M$. The remaining M rows are defined by the connectivity of the second group and equal to $M + \gamma N$. As a result, the minimal cluster partition has two colors. The corresponding cluster synchronization manifold

$$\begin{aligned} D(2) = \{&\Theta_1 = \cdots = \Theta_N = \Theta, \quad \dot\Theta_1 = \cdots \dot\Theta_N = \dot\Theta, \\ &\Phi_1 = \cdots = \Phi_M = \Phi, \quad \dot\Phi_1 = \cdots \dot\Phi_M = \dot\Phi\} \end{aligned} \tag{4}$$

defines two clusters of synchrony. As the two groups of oscillators are formed by all symmetrical all-to-all networks, all other combinations of cluster partitions within the two clusters are also possible. This includes so-called chimeras,[43] where the first group of N oscillators is completely synchronized, and all M oscillators from the second group are desynchronized; this state is defined by the cluster synchronization manifold $D(M+1) = \{\Theta_1 = \cdots = \Theta_N, \quad \dot\Theta_1 = \cdots \dot\Theta_N, \quad \Phi_1, \ldots, \Phi_M, \dot\Phi_1, \ldots, \dot\Phi_M\}$. Note that complete synchronization is impossible in the network (2) as $N \neq M$ and the equal row sum constraint is not respected.

In the following, we will focus on the dynamics on the two-cluster synchronization manifold $D(2)$ and the conditions of its transversal stability.

B. Dynamics on the cluster manifold

1. Transformation to the pendulum equation

The dynamics on the manifold $D(2)$ is defined by the following 4D system:

$$\begin{aligned} \beta\ddot\Theta + \dot\Theta &= -N\sin\alpha + \gamma M \sin(\Phi - \Theta - \alpha) \\ \beta\ddot\Phi + \dot\Phi &= -M\sin\alpha + \gamma N \sin(\Theta - \Phi - \alpha) \end{aligned} \tag{5}$$

obtained from the system (2) by omitting the subscripts i, j, and k.

For convenience, we rotate the coordinate frame and introduce new variables

$$\begin{aligned} x &= \Phi - \Theta \\ y &= \Theta + \kappa\Phi, \text{ where } \kappa = M/N < 1. \end{aligned} \tag{6}$$

The addition of the factor κ to the standard change of basis for the difference and sum variables is not necessary; however, it will make the sum variable y strictly decreasing, therefore making the analysis simpler.

In terms of x and y, the system (5) can be rewritten as follows:

$$\beta\ddot x + \dot x = (N - M)\sin\alpha - \gamma(N\sin(x+\alpha) + M\sin(x-\alpha)), \tag{7a}$$

$$\beta\ddot y + \dot y = -(N + \kappa M)\sin\alpha + \gamma M(\sin(x-\alpha) - \sin(x+\alpha)). \tag{7b}$$

We use the following trigonometric formula to simplify Equation (7a):

$$\begin{aligned} &N\sin(x+\alpha) + M\sin(x-\alpha) \\ &\quad = ((M+N)\cos\alpha)\sin x + ((N-M)\sin\alpha)\cos x \\ &\quad = R\sin(x+\delta), \end{aligned}$$

where $R = \gamma\sqrt{N^2 + M^2 + 2MN\cos 2\alpha}$ and the angle δ is introduced to make the expression more manageable, with $\cos\delta = \frac{N+M}{R}\cos\alpha$ and $\sin\delta = \frac{N-M}{R}\sin\alpha$, yielding $\tan\delta = \frac{N-M}{N+M}\tan\alpha = \frac{1-\kappa}{1+\kappa}\tan\alpha$. Similarly simplifying the right-hand side of (7b), we turn the system (7a) and (7b) into the following form:

$$\beta\ddot x + \dot x = \Omega - R\sin(x+\delta), \tag{8a}$$

$$\beta\ddot y + \dot y = -(\tilde\Omega + 2\gamma M\cos x)\sin\alpha, \tag{8b}$$

where $\Omega = (N-M)\sin\alpha, \tilde\Omega = \frac{N^2+M^2}{N}$, and $\delta = \arctan\left(\frac{1-\kappa}{1+\kappa}\tan\alpha\right)$, with $\kappa = M/N$.

The shift $x + \delta \to x$ transforms the system (8a) and (8b) into the form

$$\beta\ddot x + \dot x + R\sin(x) = \Omega, \tag{9a}$$

$$\beta\ddot y + \dot y = -(\tilde\Omega + 2\gamma M\cos(x-\delta))\sin\alpha. \tag{9b}$$

Note that Equation (9a), governing the difference dynamics between the clusters, does not depend of the sum variable y, such that Equation (9a) drives Equation (9b). Remarkably, Equation (9a) is the equation of a pendulum, with a constant torque Ω,[55] as well as the model of a shunted Josephson junction.[60] Its dynamics on the cylinder $(x \bmod 2\pi, \dot x = v)$ are known to exhibit various interesting dynamical regimes, including bistability where a stable equilibrium co-exists with a stable limit cycle. Figure 1 illustrates the well-known

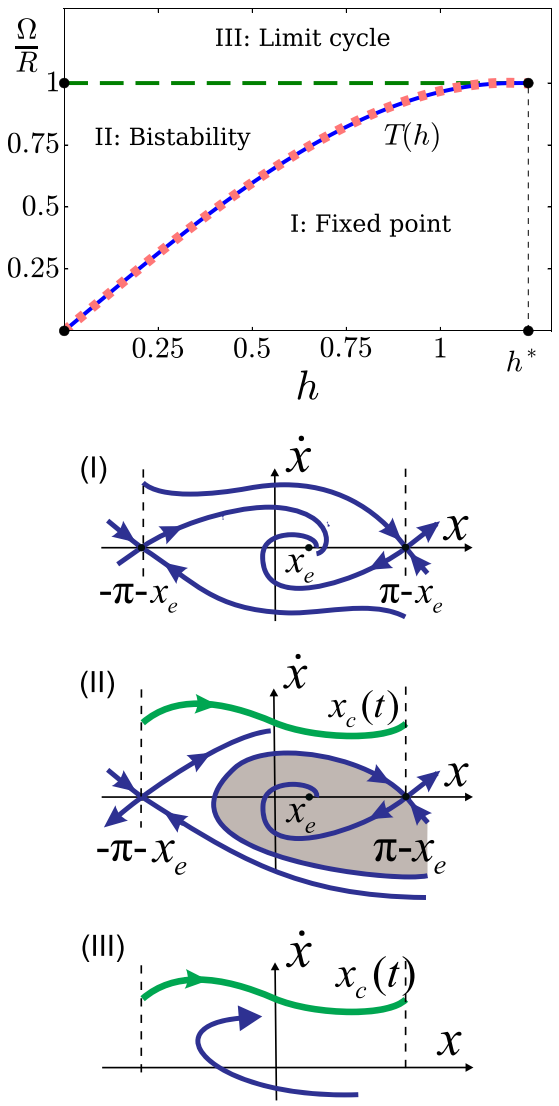

FIG. 1. Bifurcation diagram $(h, \frac{\Omega}{R})$. The saddle-node (green dashed) horizontal line and the Tricomi (blue solid) curve $T(h)$ divide the diagram into regions I–III. The Tricomi curve, corresponding to a homoclinic bifurcation of the saddle, is calculated numerically. Its nearly perfect analytical approximation $\frac{\Omega}{R} = T(h) = \frac{4}{\pi}h - 0.305h^3$, used in the bistability condition (18), is depicted by the red dashed line. (I–III). Schematic phase portraits. In (II), the stable limit cycle $x_c(t)$ co-exists with the stable fixed point x_e. The shaded area is the basin of attraction of the fixed point x_e.

stability diagram[58,60] that indicates possible dynamics as a function of bifurcation parameters Ω, R, and β. Two bifurcation curves separate the stability diagram into three regions of parameters. The curve $\Omega/R = 1$ corresponds to a saddle-node bifurcation of equilibria. The curve $\Omega/R = T(h)$ with $h = 1/\sqrt{\beta R}$ is the Tricomi curve[57] that indicates a homoclinic bifurcation of the saddle where the homoclinic orbit encircles the cylinder and forms a saddle connection. The two curves meet at $h^* \approx 1.22$.[55,59] While the closed-form derivation of the Tricomi curve is not available, we suggest the following nonlinear function $T(h)$ as an approximation of the Tricomi curve:

$$T(h) = \frac{4}{\pi}h - 0.305h^3 = \frac{4}{\pi\sqrt{\beta R}} - 0.305(\beta R)^{-3/2}. \quad (10)$$

This approximation matches the numerically calculated Tricomi curve remarkably well (see Fig. 1) and will be used for the derivation of the bistability conditions of cluster synchrony in Statement 1.

The three stability regions of parameters in the pendulum equation (8a) are as follows.

a. Region I: A stable equilibrium.

$$\frac{\Omega}{R} < \begin{cases} T(h), & 0 < h < h^* \\ 1, & h > h^*. \end{cases} \quad (11)$$

In this region, system (8a) has two fixed points on the cylinder: a saddle at $x = \pi - \arcsin\frac{\Omega}{R} - \delta$ and a stable equilibrium (node or focus) at

$$x_e = \arcsin\frac{\Omega}{R} - \delta. \quad (12)$$

b. Region II: Co-existence.

$$T(h) < \frac{\Omega}{R} < 1, \quad 0 < h < h^*. \quad (13)$$

Here, the stable equilibrium at x_e co-exists with a stable limit cycle which emerged from the homoclinic orbit of the saddle at $\Omega/R = T(h)$. $x_c(t)$ denotes the x-coordinate of the stable limit cycle. The attraction basins of the stable equilibrium and the limit cycle are separated by a stable manifold of the saddle (Fig. 1).

c. Region III: A globally stable limit cycle. For $\frac{\Omega}{R} > 1$, system (8a) only has a globally stable limit cycle as the saddle and the stable node have disappeared via the saddle-node bifurcation at $\Omega/R = 1$. The stable limit cycle corresponds to rotation around the cylinder.

Equation (8b) for the sums of the cluster coordinates is driven in (8b) via $x(t)$. Therefore, as long as $\tilde{\Omega} + 2\gamma M \cos x > 0$, any solution of (8b) eventually satisfies $\dot{y} < 0$ and $y(t)$ monotonically decreases in time. In particular, the time-dependent solution $(y_e, \dot{y}_e)$ of (8b), corresponding to the stable fixed point x_e in (8a), is obtained by integrating (8b) such that

$$y_e = -([(\tilde{\Omega} + 2M\gamma\cos x_e)\sin\alpha]t + y_0), \quad (14)$$

where y_0 is a constant of integration. The solution $(y_c, \dot{y}_c)$, corresponding to the limit cycle x_c in (8b), is not given explicitly.

Thus, we can conclude that three distinct dynamics of system (8a) in regions I–III yield the three dynamical regimes on the cluster manifold $D(2)$ in the network system (2).

2. Cluster phase shifts

a. Constant phase shift (region I). Governed by the phases Φ and Θ, two clusters of synchrony have a constant phase shift $\Phi_e - \Theta_e = x_e$, where x_e is the coordinate of the stable equilibrium of the pendulum system (8a) and defined in (12). It follows from (5) and (6) that the cluster phases at x_e are defined by

$$\Theta_e = \frac{y_e - \kappa x_e}{1+\kappa}, \quad \Phi_e = \frac{y_e + x_e}{1+\kappa} = \Theta_e + x_e, \tag{15}$$

where y_e is defined in (14).

As the phase shift is constant, the rotation frequencies of the two clusters become equal and are defined, according to the system (5), by

$$\begin{aligned}\dot{\Theta} &= -N\sin\alpha + \gamma M \sin(x_e - \alpha) = \dot{\Phi} \\ &= -M\sin\alpha - \gamma N \sin(x_e + \alpha).\end{aligned} \tag{16}$$

b. Co-existence of constant and oscillating phase shifts (region II). The co-existence of the stable equilibrium and the limit cycle in system (8a) yields the bistability of the cluster regimes. Here, the phase shift can remain constant at x_e or periodically oscillate such that $\Phi - \Theta = x_c(t)$, which is governed by the stable limit cycle. The realization of one of the cluster regimes depends on initial conditions.

c. Oscillating phase shift (region III). Defined by the globally stable limit cycle in (8a), the phase difference between the clusters, establishing from any conditions on the cluster manifold M, periodically oscillates such that

$$\Theta_c = \frac{y_c - \kappa x_c}{1+\kappa}, \quad \Phi_c = \frac{y_c + x_c}{1+\kappa} = \Theta_c + x_c(t)\,. \tag{17}$$

The bistability condition (13) can be expressed in terms of the original parameters of the network system (2). This leads to the following assertion.

Statement 1: *The constant and oscillating phase shifts* $x = \Phi - \Theta$ *between two clusters on the cluster manifold D(N) in the network system (2) co-exist if*

$$\begin{aligned}\alpha_{\mathrm{TR}} &= \arctan\frac{1+\kappa}{1-\kappa}\frac{\gamma T(h)}{\sqrt{1-\left(\gamma T(h)\right)^2}} < \alpha \\ &< \arctan\frac{1+\kappa}{1-\kappa}\frac{\gamma}{\sqrt{1-\gamma^2}} = \alpha^*,\end{aligned} \tag{18}$$

where $\kappa = M/N$, $T(h) = \frac{4}{\pi\sqrt{\beta R}} - 0.305(\beta R)^{-3/2}$, *and* $R = \gamma\sqrt{N^2 + M^2 + 2MN\cos 2\alpha}$. *The left hand side of the inequality (18) is defined by* α_{TR} *which corresponds to the Tricomi curve (11). The right hand side is determined by the critical value* α^*, *for which system (8a) undergoes the saddle-node bifurcation at* $\frac{\Omega}{R} = 1$, *where* $\Omega = (N-M)\sin\alpha$. *Condition (18) can also be cast in the alternative, more compact form*

$$\frac{4}{\pi\sqrt{\beta R}} - 0.305(\beta R)^{-3/2} < \frac{\Omega}{R} < 1. \tag{19}$$

In Section IV, we will derive conditions on the stability of the clusters. In particular, we will combine the stability conditions with the co-existence condition of Statement 1 to determine the parameter regions of two co-existing stable cluster regimes with constant and oscillating shifts. We will also discuss conditions for the emergence of chimeras when one cluster of oscillators remains stable while the other cluster disintegrates.

IV. STABILITY OF CLUSTERS

Linearizing the network system (2) about the synchronous cluster solution (4) $(\Theta, \dot{\Theta}, \Phi, \dot{\Phi})$, we obtain the variational equations for the local stability of the cluster manifold $D(2)$

$$\begin{aligned}\beta\ddot{\xi}_i + \dot{\xi}_i &= -(N\cos\alpha + \gamma M\cos(x_s - \alpha))\xi_i \\ &\quad + \cos\alpha\sum_{j=1}^{N}\xi_j + \gamma\cos(x_s-\alpha)\sum_{j=1}^{M}\eta_j, \quad i = 1,\ldots,N \\ \beta\ddot{\eta}_k + \dot{\eta}_k &= -(M\cos\alpha + \gamma N\cos(x_s+\alpha))\eta_k \\ &\quad + \cos\alpha\sum_{j=1}^{M}\eta_j + \gamma\cos(x_s+\alpha)\sum_{j=1}^{N}\xi_j, \quad k = 1,\ldots,M.\end{aligned} \tag{20}$$

Here, ξ_i is an infinitesimal perturbation of the ith oscillator's synchronous solution in the larger N-cluster, and η_k corresponds to the smaller M-cluster. x is the cluster phase shift as defined above. System (20) can be rewritten in the matrix form

$$\beta\ddot{V} + \dot{V} = AV, \tag{21}$$

where vector $V = \mathrm{column}(\xi_1,\ldots,\xi_N,\eta_1,\ldots,\eta_M)$. Matrix A is the Jacobian

$$A = \begin{pmatrix} cJ_{N,N} - (Nc + Mc^-)I_N & c^-J_{N,M} \\ c^+J_{M,N} & cJ_{M,M} - (Mc + Nc^+)I_M \end{pmatrix}, \tag{22}$$

where $c = \cos\alpha$, $c^- = \gamma\cos(x_s - \alpha)$, $c^+ = \gamma\cos(x_s+\alpha)$, I_N and I_M are identity matrices, and $J_{N,N}$, $J_{N,M}$, and $J_{M,N}$ are all-ones matrices.

A. Stability along the cluster manifold

The $(N+M)\times(N+M)$ Jacobian A has equal zero-row sums. Therefore, it contains one zero eigenvalue that corresponds to Equation (8b), which governs the rotating frame coordinate y on the cluster manifold $D(2)$. An eigenvector $V_{\mathrm{syn}} = \mathrm{column}(\underbrace{\xi,\ldots,\xi}_{N},\underbrace{\eta,\ldots,\eta}_{M})$ determines the direction along the cluster manifold $D(2)$. The corresponding eigenvalue

$$\begin{aligned}\lambda_s &= -Nc^+ - Mc^- \\ &= -\gamma(N\cos(x_s+\alpha) + M\cos(x_s-\alpha)), \quad s = e,c\end{aligned} \tag{23}$$

defines the stability of the fixed point $x = x_e$ or the limit cycle $x = x_c(t)$ in the pendulum equation (8a) which governs the dynamics of the cluster shift on the cluster manifold $D(2)$.

Case I: Fixed point x_e.

If the dynamics on the cluster manifold is governed by the fixed point $x_e = \arcsin\frac{\Omega}{R} - \delta$ (cf. (12)), the stability of

the constant phase shift between the two clusters is defined via the eigenvalue (23) such that

$$-\lambda_e = \gamma(N\cos(x_e+\alpha) + M\cos(x_e-\alpha)) > 0. \tag{24}$$

This condition holds true as long as $\frac{\Omega}{R} < 1$ and the stable fixed point exists in region I (cf. Fig. 1).

Case II: Limit cycle $x_c(t)$.

In this case, the eigenvalue λ_c is defined by the time-varying phase shift $x_c(t)$. The stability of the limit cycle is defined by the variational equation

$$\beta\ddot{\zeta} + \dot{\zeta} - \lambda_c(t)\zeta = 0, \tag{25}$$

written for the perturbations ζ to the limit cycle of system (7a). The stability of the cycle in Equation (25) is defined by the Lyapunov characteristic exponents. One of the exponents is zero and corresponds to the direction along the limit cycle, whereas the other is negative as the divergence of the vector field of (7a) is negative, $\mathrm{div}F(x=v,\dot{v}) = -1/\beta < 0$. Therefore, the limit cycle x_c is stable and determines the stability of the synchronous solution on the cluster manifold $D(2)$.

B. Transversal stability

To demonstrate that the synchronous clusters can stably appear in the network (2), we shall prove the transversal stability of the cluster manifold $D(2)$. We introduce the difference variables

$$\begin{aligned} u_i &= \xi_i - \xi_{i+1}, \quad i = 1,\ldots,N-1 \\ w_k &= \eta_k - \eta_{k+1}, \quad k = 1,\ldots,M-1, \end{aligned} \tag{26}$$

whose convergence to zero will imply the transversal stability of $D(2)$. Subtracting the $(i+1)$-th $[(k+1)$-th] equation from the ith [kth] equation in system (21) and (22), we obtain the variational equations for the transversal stability

$$\beta\ddot{u}_i + \dot{u}_i + q_1 u_i = 0, \quad i = 1,\ldots,N-1, \tag{27a}$$

$$\beta\ddot{w}_i + \dot{w}_i + q_2 w_i = 0, \quad i = 1,\ldots,M-1, \tag{27b}$$

where

$$q_1 = Nc + Mc^- = N\cos\alpha + \gamma M\cos(x_s-\alpha), \tag{28a}$$

$$q_2 = Nc^+ + Mc = N\gamma\cos(x_s+\alpha) + M\cos\alpha. \tag{28b}$$

Here, q_1 and q_2 are eigenvalues of the Jacobian A in (22) which have multiplicities $N-1$ and $M-1$, respectively. Note that Equations (28a) and (28b) are uncoupled. The analysis of the stability equations (28a) and (28b) leads to the following assertions.

Theorem 1. [Stability of the cluster solution with a constant phase shift].

Let the parameters satisfy the condition $\Omega/R < 1$, then the cluster solution (4) $(\Theta,\dot{\Theta},\Phi,\dot{\Phi})$ with the constant phase shift x_e is locally stable to transversal perturbations iff

$$\alpha < \alpha^{\mathrm{cr}}, \tag{29}$$

where the critical value α^{cr} is the solution of the equation

$$q_2 = \gamma\cos(x_e+\alpha) + \kappa\cos\alpha = 0. \tag{30}$$

Here, $\gamma \in (0,1)$ is the coupling ratio, x_e is defined via (12), $\kappa = M/N$, and $\alpha \in [0, \alpha^*)$, where $\alpha^* = \arctan\frac{1+\kappa}{1-\kappa}\frac{\gamma}{\sqrt{1-\gamma^2}}$ (see (18)). Positive values of q_2 correspond to $\alpha < \alpha^{cr}$ and define the stability of the cluster solution.

Proof. The condition $\Omega/R < 1$ implies that the pendulum equation (8a), governing the dynamics of the phase shift x on the cluster manifold $D(2)$, has a stable equilibrium point $x_e = \arcsin\frac{\Omega}{R} - \delta$ (see Fig. 1). Therefore, functions (28a) and (28b), q_1 and q_2, must be evaluated at x_e. The stability of the variational system (27a) and (27b) is guaranteed iff

$$q_1 = \cos\alpha + \gamma\kappa\cos(x_e-\alpha) > 0, \tag{31a}$$

$$q_2 = \gamma\cos(x_e+\alpha) + \kappa\cos\alpha > 0. \tag{31b}$$

This is due to the fact that $q_{1,2} > 0$ is required for the real parts of the roots of the characteristic equations $\beta s^2 + s + q_{1,2} = 0$ for (27a) and (27b) to be negative. Note that $\cos\alpha > 0$ and $\cos(x_e-\alpha) > 0$ for $\alpha \in [0, \pi/2)$ in (31a), and therefore $q_1 > 0$.

The phase shift x_e is a monotonically increasing function of α. Therefore, the function q_2 monotonically decreases and can become negative when increasing α. As a result, there is a critical value α^{cr} for which q_2 becomes 0. Finding α^{cr} amounts to solving $q_2 = \gamma\cos(x_e+\alpha) + \kappa\cos\alpha = 0$. While this equation cannot be solved for α in closed form, α^{cr} can be directly calculated for given values of N, M, and γ. This concludes the proof. □

Corollary 1. [Sufficient condition]. *If the relative size of the two clusters $\kappa = M/N$ satisfies the following sufficient condition*

$$\kappa < 1 - 2\gamma^2, \tag{32}$$

then the cluster solution $(\Theta,\dot{\Theta},\Phi,\dot{\Phi})$ is locally stable to transversal perturbations for any $\alpha \in [0, \alpha^*)$.

Proof. The maximum value of α^{cr} is bounded by α^* that corresponds to the saddle-node bifurcation of the fixed point x_e at $\Omega/R = 1$. Therefore, this bound gives the constraints on γ and κ that can be calculated from

$$q_2 = \gamma\cos(x_e+\alpha^*) + \kappa\cos\alpha^* > 0. \tag{33}$$

As $x_e(\alpha^*) = \pi/2 - \arcsin\gamma = \pi/2 - \arctan\frac{\gamma}{\sqrt{1-\gamma^2}}$, we get $\cos(x_e+\alpha^*) = \sin(\arcsin\gamma - \alpha^*) = \gamma\cos\alpha^* - \sqrt{1-\gamma^2}\sin\alpha^*$. Therefore, the condition (33) can be rewritten as follows:

$$q_2 = (\gamma^2+\kappa)\cos\alpha^* - \gamma\sqrt{1-\gamma^2}\sin\alpha^* > 0. \tag{34}$$

It further transforms into

$$\tan\alpha^* < \frac{\gamma^2+\kappa}{\gamma\sqrt{1-\gamma^2}}. \tag{35}$$

At the same time $\tan\alpha^* = \frac{1+\kappa}{1-\kappa}\frac{\gamma}{\sqrt{1-\gamma^2}}$ (see Statement 1), therefore, condition (35) becomes

$$\frac{1+\kappa}{1-\kappa}\frac{\gamma}{\sqrt{1-\gamma^2}} < \frac{\gamma^2+\kappa}{\gamma\sqrt{1-\gamma^2}} \tag{36}$$

and yields the sufficient condition $\kappa < 1 - 2\gamma^2$. This concludes the proof of Corollary 1. □

Figure 2 illustrates the conditions of Theorem 1 for $q_2 > 0$ and demonstrates that the stable cluster with a constant shift exists in a wide region of parameters α, γ, κ. Notice that α^{cr}, which separates the stability and instability regions, coincides with α^* for a significant (lower) part of the curve α^* (see Fig. 2(b)). Hence, in this region of $\alpha \in [0, 1.26056)$ and $\gamma \in [0, 0.3275)$, the cluster with a constant shift, defined by the stable fixed point x_e of Equation (7a), remains stable as long as it exists. For values $\gamma \geq 0.3275$, the cluster becomes unstable at $\alpha^{cr} < \alpha^*$ and remains unstable until it ceases to exist at α^* (see the dark blue instability region in Fig. 2(b)).

Remark 1. If the size of the cluster groups is equal so $N = M$, then cluster synchronization turns into complete synchronization with phase shift $x_e = 0$. As a result, the stability condition (29) in Theorem 1 holds true for any $\alpha \in [0, \alpha^*)$, so complete synchronization is always (locally) stable. In regard to Fig. 2(a), the corresponding horizontal cut at $\kappa = M/N = 1$ contains no unstable region, and $q_2 > 0$ for any $\alpha \in [0, \alpha^*)$ (this top cut is not shown for a better visibility of lower cuts $\kappa \in [0.1, 0.9]$).

Remark 2. If $\gamma = \kappa$, then α^{cr} from the stability condition (29) can be explicitly calculated and equals $\alpha^{cr} = \pi/2 - x_e/2$. This follows from Equation (30) where γ can be replaced by $\kappa = \frac{M}{N}$. Therefore, Equation (30) simplifies to $\cos(x_e + \alpha) + \cos\alpha = 2\cos\frac{x_e+\alpha}{2}\cos\frac{x_e-\alpha}{2} = 0$ which holds true if $\alpha = \alpha^{cr} = \pi/2 - x_e/2$.

Remark 3. [Relation to the stability of chimeras]. When condition (29) is violated such that the function $q_2 < 0$, the two-cluster pattern loses its stability (see Fig. 2). As it follows from the variational equations (27a) and (27b), the stability of the N-cluster of synchronous oscillators $(\Theta, \dot{\Theta})$ is determined by the condition $q_1 > 0$ which holds true for any $\alpha \in [0, \pi/2)$, independent from the sign of q_2. Therefore, when q_2 changes sign from positive to negative, the trivial fixed point of the variation equations (27a) and (27b), which corresponds to the cluster manifold, becomes a saddle. This saddle point has a stable manifold of dimension $2N + M$ and an unstable manifold of dimension M, where the $2N$ stable directions correspond to the variables of the first N oscillators and are defined by the condition $q_1 > 0$. At the same time, the M unstable directions are determined by the condition $q_2 < 0$, which implies transversal instability of the M variables of the oscillators from the second cluster. A trajectory, starting close to the stable manifold of the saddle point may remain close to it, giving rise to a transient chimera, where the first cluster persists for a some fairly long amount of time, especially in a large network. This argument comes from the rigorous conditions on the stability/instability of the cluster solution (4) $(\Theta, \dot{\Theta}, \Phi, \dot{\Phi})$ whose stability along the cluster manifold $D(2)$ is proven. At the same time, a rigorous proof of the stability of a non-transient chimera state $D(M+1) = \{\Theta_1 = \cdots = \Theta_N, \dot{\Theta}_1 = \cdots \dot{\Theta}_N, \Phi_1, \ldots, \Phi_M, \dot{\Phi}_1, \ldots, \dot{\Phi}_M\}$ via the stability of the first cluster oscillators' variables remains elusive. This is due to the fact that the stability of the chimera state solution along the chimera manifold $D(M+1)$ cannot be rigorously assessed via the 2D equation for the dynamics of the phase shift (8a) but must be proven through the full $2 \times (M+1)$ system, similar to (5), where Φ is replaced with $\Phi_1, \ldots, \Phi_M$. Although, our numerical simulations indicate the emergence of non-transient chimeras (see Fig. 5), where the N-cluster never disintegrates and remains stable.

Theorem 2. [Stability of the breathing cluster solution] (sufficient conditions). *Let the parameters satisfy the condition: $\Omega/R > T(h)$ (see Fig. 1) such that the system (8a) has a stable limit cycle which determines the oscillating phase shift $x_c(t)$ between two clusters. Then, the cluster solution (4) $(\Theta, \dot{\Theta}, \Phi, \dot{\Phi})$ with the phase shift x_c in the network system (2) is locally stable to transversal perturbations if*

$$\kappa \cos\alpha > \gamma, \tag{37a}$$

$$1 - 4\beta N(k\cos\alpha - \gamma) > 0. \tag{37b}$$

Proof. As in the proof of Theorem 1, we should find parameter regions for the stability of the variational equations (27a) and (27b). In contrast to the previous case of the constant phase shift x_e, the oscillating phase shift $x_c(t)$ makes q_1 and q_2 time-varying periodic functions, and therefore, the variational equations (27a) and (27b) contain time-varying coefficients. While the precise bounds on the stability of (27a) and (27b) can be numerically assessed via the calculation of the Lyapunov exponents, we derive analytical estimates as follows. As in the case of the constant phase shift x_e, the necessary condition for the stability of (27a) and (27b) is $q_1(x_c(t)) > 0$ and $q_2(x_c(t)) > 0$. In this case, these two

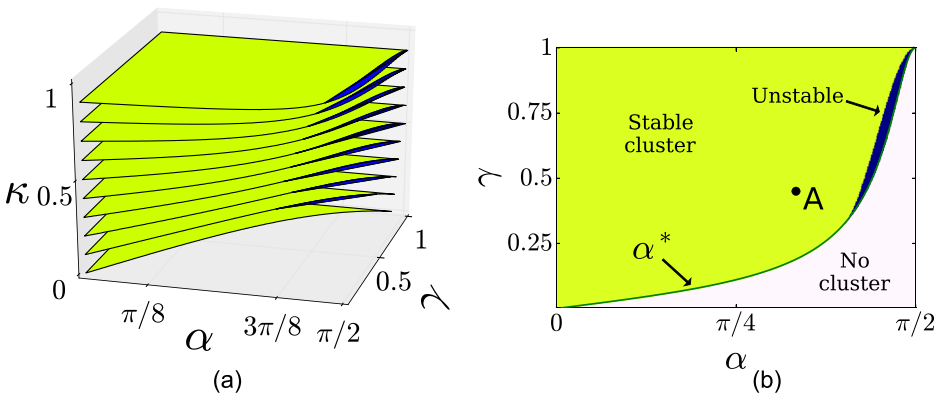

FIG. 2. Illustration of the stability condition $q_2 = \gamma\cos(x_e + \alpha) + \kappa\cos\alpha > 0$ in Theorem 1. Yellow (light) regions are defined by $q_2 > 0$ and correspond to the stable cluster with a constant shift. Instability regions with $q_2 < 0$ are depicted in dark blue. The cluster with a constant shift does not exist in white regions. (a). 3D diagram with 2D cuts at various discrete $\kappa = M/N$. (b). 2D cut at $\kappa = 0.8$. The curve α^* separates the regions of existence (yellow/blue) and non-existence (white). Point A corresponds to the parameters used in Fig. 4.

inequalities must be fulfilled for any time instant during the period of the cycle $x_c(t)$. The condition $q_1 = N\cos\alpha + \gamma M\cos(x_c(t)-\alpha) > 0$ can be estimated via the worst-case stability scenario where $\cos(x_c(t)-\alpha) = -1$. That is, $q_1(x_c(t)) > 0\,\forall t$ if $\cos\alpha > \kappa\gamma$. Similarly, we get the bound on $q_2(x_c(t)) > 0\,\forall t$ if $\cos\alpha > \gamma/\kappa$. As $\kappa < 1$, the condition for q_2 also guarantees the condition for q_1. This gives bound (37a).

While bound (37a) alone would be sufficient if q_1 and q_2 were constant, increasing β can destabilize the variational equations (27a) and (27b) with periodically varying coefficients. The destabilizing contribution of β can be assessed via a simple criterion that the discriminants D_{q_1,q_2} of the corresponding characteristic equations $\beta s^2 + s + q_{1,2}(x_c(t)) = 0$ are positive.[61] In simple words, this sufficient condition implies that as long as the origin remains a stable node fixed point of variational equations (27a) and (27b) for any fixed instant of time and never turns into a degenerate node or a focus, the variational equations (27a) and (27b) with time-varying parameters are stable. For the worst case of $\cos(x_c(t)+\alpha) = -1$, the condition on $D_{q_2} = 1 - 4\beta q_2 > 0$ yields bound (37b). This bound also includes the bound for $D_{q_1} > 0$. □

Remark 4. The use of the worst-case stability approximation $\cos(x_c(t)+\alpha) = -1$ yields a very conservative range of values κ, γ, and α. It implies that the trivial fixed point of the variational equations (27a) and (27b) with time-varying coefficients is stable for any value of $x_c(t)$. In reality, this does not have to be the case as long as its overall stability over the period of the limit cycle $x_c(t)$ is preserved such that its Lyapunov exponents remain negative. As a result, the sufficient conditions (37a) and (37b) should be considered as a proof of concept, giving an analytical proof for the stability and feasibility of a breathing cluster in the network system (2) (see Fig. 3 for the comparison with the numerically assessed region of stability).

Statement 2 [Bistability conditions]: *Combining the co-existence condition (18) of Statement 1 with the stability criteria of Theorems 1 and 2, yields sufficient conditions on the co-existence of two stable patterns of synchrony with constant and oscillating phase shifts between two clusters*.

In the following, we provide a numerical example of these bistable regimes and hysteretic transitions between them in a small network (2).

V. NUMERICAL EXAMPLE

As the emergence of stable clusters and chimeras is easier to demonstrate in large Kuramoto networks without[38,43] and with inertia,[49] where the dynamics is close to its mean-field approximation, we knowingly choose the harder case of a small network (2) with $N = 5$ and $M = 4$ as our numerical example. Along with $\kappa = M/N = 0.8$, we fix parameter $\gamma = 0.45$ and study the dynamics of clusters as a function of α and β.

Figure 3 demonstrates how inertia β affects hysteretic transitions between the co-existing clusters. When inertia is small ($\beta = 0.1$), the network is mono-stable such that the

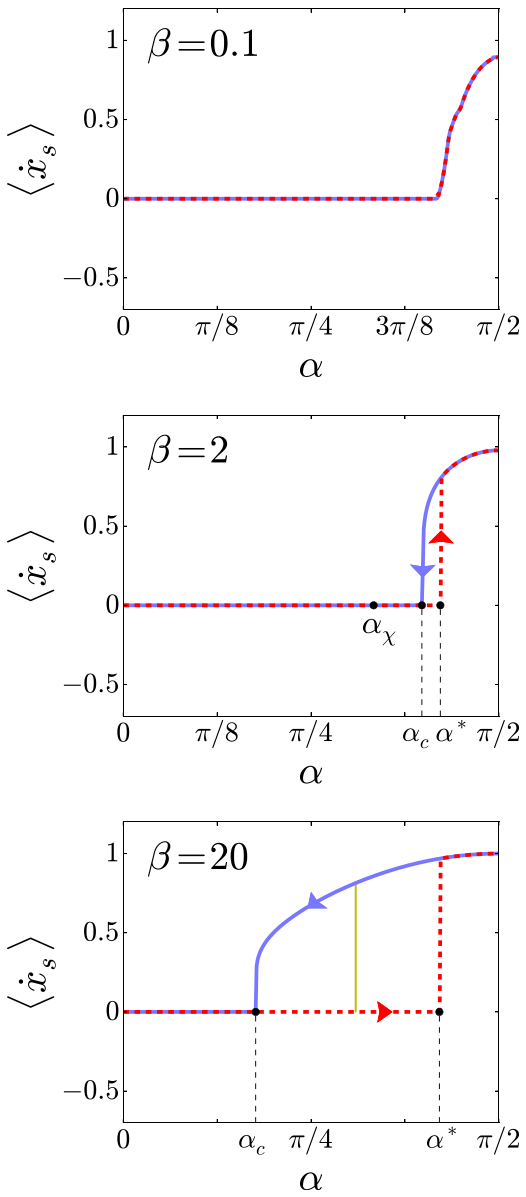

FIG. 3. Hysteretic transitions as a function of α and β. The cluster with a constant shift is indicated by the zero derivative of phase shift $\langle\dot{x}_s\rangle$. Non-zero averaged derivative $\langle\dot{x}_s\rangle$ indicates the breathing cluster with an oscillating shift. The red dashed (blue solid) line corresponds to the direction of increasing (decreasing) α. $\beta = 0.1$: The clusters do not co-exist. $\beta = 2$: Clusters co-exist in the region (α_c, α^*). Point α_χ corresponds to the co-existence of the cluster with a constant shift and a stable chimera depicted in Fig. 5. $\beta = 20$: Increased inertia β enlarges the bistability region. The range $[\alpha_c = 0.5537, \alpha^* = 1.3273]$ matches the analytical condition of Statement 1. The thin vertical light stripe corresponds to the sufficient condition of Theorem 2.

breathing cluster emerges after the cluster with a constant shift disintegrates. Our simulations for $\beta = 2$ and $\beta = 20$ indicate that inertia promotes bistability and extends the range of α where the two clusters stably co-exist. Notice that the cluster with a constant shift loses its stability at α^* which corresponds to a saddle-node bifurcation of the fixed point in the pendulum equation (8a) (see Fig. 2). Therefore, this cluster is stable as long as it exists. When α decreases, the breathing cluster loses its stability at α_c which coincides with α_{TR}, where the limit cycle $x_c(t)$ merges into a homoclinic loop of the saddle and disappears with further decrease of α

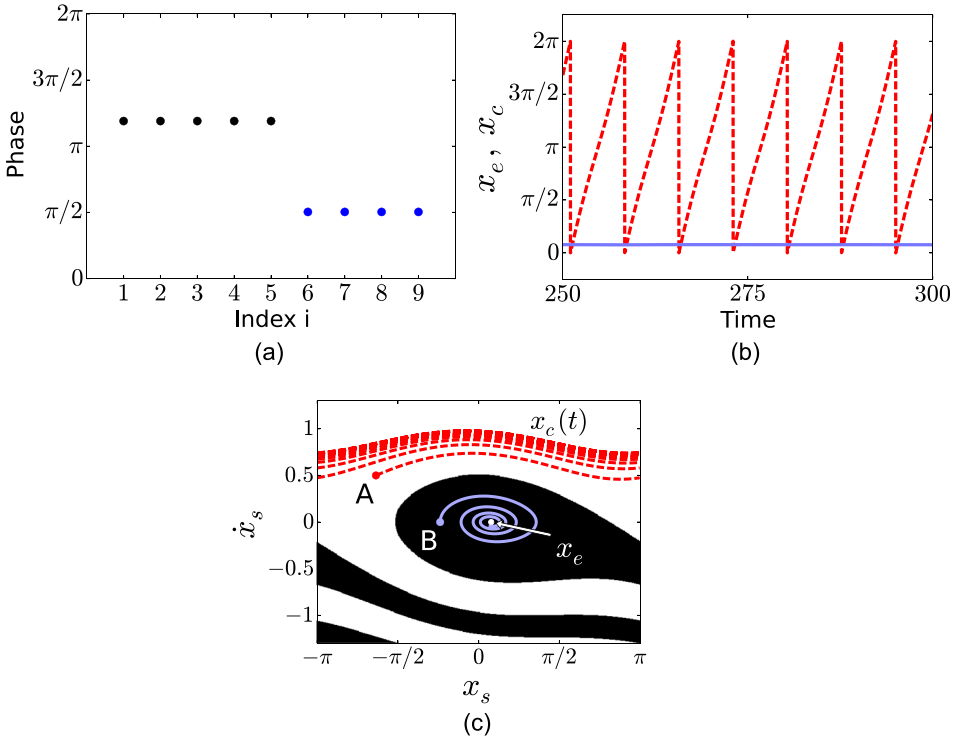

FIG. 4. (a). Snapshot of the synchronized two-cluster pattern in the network (2) for $\alpha = \pi/3$ and $\beta = 20$. Initial conditions are chosen close to the cluster manifold and correspond to the breathing cluster pattern. (b). Corresponding time series of the co-existing phase shifts x_e and $x_c(t)$, robustly appearing from non-identical random initiation conditions, close to the cluster manifold. (c). Co-existence of the constant (x_e) and oscillating phase shifts ($x_c(t)$), determined by the fixed point (depicted in white) and the stable limit cycle (depicted in red), respectively. Initial conditions are chosen on the cluster manifold. Trajectories starting from initial conditions A and B converge to different attractors (the fixed point and limit cycle). Basins of attraction of the fixed point and the limit cycle are shown in black and white, respectively.

(cf. condition (18) in Statement 1). Therefore, similarly to the cluster with a constant shift, the breathing cluster remains stable as long as it is present. The values $\alpha_c = 1.3312$ for $\beta = 2$ and $\alpha_c = 0.5537$ for $\beta = 20$ match the values of the analytical bound (18) of Theorem 1 remarkably well. As a result, the co-existence range of α, predicted in Statement 1, coincides with the actual bistability range, observed in Fig. 3.

We have also verified the sufficient conditions of Theorem 2 in the worst case of large inertia ($\beta = 20$). The sufficient conditions (37a) and (37b) for the stability of the breathing cluster yield a narrow region $0.9700 < \alpha < 0.9733$ which is depicted by the light thin stripe in Fig. 3. While being very conservative, this region lies inside the bistability region. In accordance with (37b), this region becomes less conservative and enlarges when β decreases.

Figure 4 gives a more detailed description of the co-existing stable clusters with a constant and periodically oscillating phase shifts for $\alpha = \pi/3$ and $\beta = 20$ (cf. point A in Fig. 2(b)). In Fig. 4(a), we present a snapshot of the established cluster pattern. The oscillators in the first five- and second four-oscillator groups synchronize within the two clusters, and there is always a phase shift between the two synchronized groups. Depending on the initial conditions, the network exhibits either the two-cluster pattern with a constant inter-cluster phase shift or a breathing two-cluster pattern where the phase shift oscillates. While the static snapshot of Fig. 4(a) does not allow for identifying the dynamics of the phase shift, it actually corresponds to the breathing cluster with the oscillating phase shift x_c, (red waveform depicted in Fig. 4(b)). Figure 4(b) indicates the bistability of the two patterns of synchrony starting from random non-equal initial conditions close to the cluster solution. Figure 4(c) shows the co-existence of the two dynamics for the phase shifts, similar to the qualitative phase portrait of Fig. 1. To explicitly define the phase shift x between the clusters, in Fig. 4(c), we set all initial conditions for the oscillators in the first five-oscillator cluster to zero, and for the oscillators in the second four-oscillator cluster to the same set of values $x, \dot{x}$. Thus, the initial difference between the cluster variable determines the initial phase shift x. Note that different initial conditions (points A and B) induce different phase shifts.

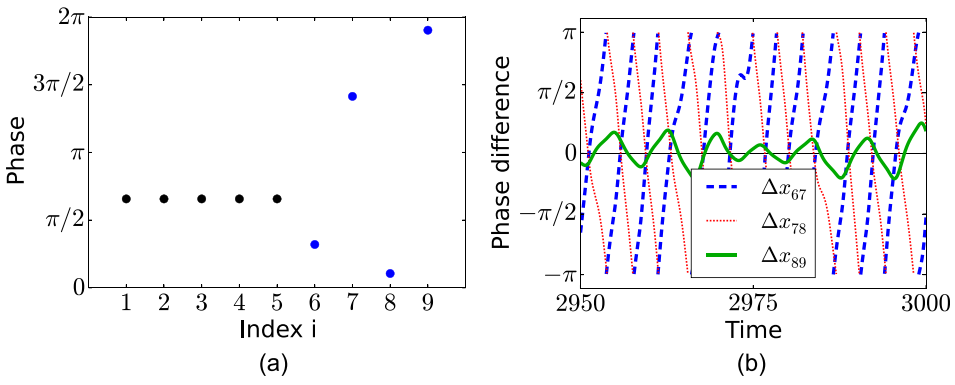

FIG. 5. (a). Snapshot of a chimera state in the network (2) for $\alpha = \alpha_\chi = \pi/3$, $\beta = 2$. (b). Time-series of the phase differences between the oscillators in the second cluster. The oscillating phase differences indicate the absence of pairwise synchrony in the second cluster, therefore showing a stable chimera.

Figure 5 shows that the breathing cluster can turn into a stable breathing chimera where the first cluster of N oscillators remains locally stable, while the second cluster of M oscillators loses its stability. This stable chimera co-exists with the cluster with a constant phase shift (see the corresponding point α_χ in Fig. 3). While we have consistently explored the range of bistability between the two clusters of synchrony both analytically and numerically, we have not performed an exhaustive search for stable chimeras in the bistability region $[\alpha_c, \alpha^*]$ (cf. Fig. 3). Finding conditions on the co-existence of both stable clusters and stable chimeras is a subject of future study.

VI. CONCLUSIONS

Rigorous analysis of the stability of cluster synchronization in complex networks of identical oscillators with symmetries has been shown to be challenging. It is typically limited to a restricted types of coupling and network topologies. This is due to the fact that the system, which determines the stability of a given multi-cluster decomposition, is high-dimensional, non-reducible, and often asymmetric. The Laplacian (diffusive) coupling with zero-row sum connectivity matrices seems to be the most difficult case for identifying cluster decompositions and proving their stability.[13–17] This is, in particular, due to complete synchronization, which is always present in unweighted, but possibly heterogeneous Laplacian networks, such that its stability often prevents the observation of co-existing stable clusters. In light of this, non-diffusive networks, such as pulse-coupled neuronal networks,[11,22] where heterogeneous node degrees, defined by different numbers of inputs received by each cell, makes complete synchronization impossible.[21] This creates distinct groups of cells with equal node degree. The equal node degree constraint is a necessary condition for cells to be in the same synchronous cluster. Together with the requirement of balanced coloring,[18–20] this constraint determines the existence of clusters of perfect symmetry and allows for effectively identifying cluster decompositions, even in large complex networks, via the combinatorial algorithms.[22,23]

In this paper, we have studied the stability of clusters in two coupled populations of identical Kuramoto oscillators with inertia. This network is essentially the two-population Kuramoto model,[37,38] proposed as a simple model of chimeras.[37] The new important modifications, which are vital for bistability of cluster patterns in our network, are (i) non-equal population sizes and (ii) the addition of inertia to the oscillator equation. Property (i) makes the existence of complete synchronization impossible such that a two-cluster pattern is the minimal cluster partition in this two-population network, although other multi-cluster partitions are also possible. Property (ii) increases the dimensionality of the intrinsic oscillator dynamics and creates a possibility for bistability of cluster patterns.

We have rigorously analyzed the dynamical properties and stability of the two-cluster pattern where the population splits into two synchronized groups, but there is always a phase shift between the groups. We have explicitly demonstrated that the dynamics of the phase shift can be bistable such that a constant phase shift co-exists with a time-varying shift which periodically changes from 0 to 2π. As a result, a two-cluster pattern with a constant shift co-exists with a breathing two-cluster pattern with an oscillating phase shift. We have derived the stability conditions for the stability of the cluster patterns. Due to the simple structure of the two-population network, the stability conditions for the variables, corresponding to the first and second populations, are independent. Therefore, the instability of synchrony within one group does not immediately imply the instability within the other group. In more rigorous terms, the cluster solution becomes a saddle such that stable transversal directions correspond to the first (larger) group of oscillators whereas unstable transversal directions correspond to the oscillators from the second (smaller) group. The stability result can be interpreted in terms of multidimensional clusters and chimeras. In large networks, high-dimensional stable manifolds of this saddle state may retain a close trajectory for a considerable amount of time, giving rise to transient chimeras.[39] It can also lead to the emergence of stable multi-cluster states, where the oscillators in the smaller population split into subgroups. Our numerical simulations, not reported in this paper, indicate these stable clusters, defined by high-dimensional cluster manifolds which are embedded into each other and contain the two-cluster manifold as a minimum cluster solution. Rigorous study of the transition from lower dimensional to high-dimensional cluster regimes, governed by the symmetry-induced embedding hierarchy[13] and accompanied by multistability of patterns of synchrony is a subject of future study.

In a more speculative way, the fulfilment of the transversal stability condition of the first cluster variables, while the transversal stability condition for the second cluster is violated, can be interpreted as a proof of a stable chimera. While the emergence of stable chimeras in the two-population network is confirmed by our numerical simulations, for this proof to be completely rigorous, one has to demonstrate the stability of the chimera solution in the longitudinal direction. This proof would require the analysis of the high-dimensional system that governs the dynamics of the chimera solution. In the case of the two-cluster solution, studied in this paper, this system is two-dimensional and allows for a rigorous analysis of its solutions. Our results, concerning small networks of phase oscillators, also support the recent observation that a network does not have to be large to exhibit stable chimeras.[43]

ACKNOWLEDGMENTS

We are thankful to the Guest Editors, Daniel Abrams, Adilson Motter, and Louis Pecora for the invitation to contribute to this Focus Issue. We are also grateful to Yaroslav Molkov for helpful discussions on approximations of the Tricomi curve. This work was supported by the National Science Foundation (USA) under Grant No. DMS-1616345 and the U.S. Army Research Office Network Science Division under Grant No. W911NF-15-1-0267 (to I.B. and B.B.) and by RSF under Grant No. 14-12-00811 and RFFI under Grant No. 15-01-08776 (to V.B.).

[1]J. Buck and E. Buck, Sci. Am. **234**, 74 (1976).
[2]J. J. Collins and I. Stewart, Science **3**, 349 (1993).
[3]M. R. Guevara, A. Shrier, and L. Glass, Am. J. Physiol. **254**, H1 (1988); PubMed number: PMID: 3337247.
[4]V. Torre, J. Theor. Biol. **61**, 55 (1976).
[5]T. I. Netoff and S. J. Schiff, J. Neurosci. **22**, 7297 (2002).
[6]L. Glass and M. C. Mackey, *From Clocks to Chaos: The Rhythms of Life* (Princeton University Press, Princeton, 1988).
[7]A. E. Motter, S. A. Myers, M. Anghel, and T. Nishikawa, Nat. Phys. **9**, 191 (2013).
[8]L. M. Pecora and T. L. Carroll, Phys. Rev. Lett. **80**, 2109 (1998).
[9]S. Boccaletti, J. Kurths, G. Osipov, D. L. Valladares, and C. S. Zhou, Phys. Rep. **366**, 1 (2002).
[10]V. N. Belykh, I. V. Belykh, and M. Hasler, Physica (Amsterdam) **195D**, 159 (2004).
[11]I. Belykh, E. de Lange, and M. Hasler, Phys. Rev. Lett. **94**, 188101 (2005).
[12]T. Nishikawa and A. E. Motter, Proc. Natl. Acad. Sci. U.S.A. **107**, 10342 (2010).
[13]V. N. Belykh, I. V. Belykh, and M. Hasler, Phys. Rev. E **62**, 6332 (2000).
[14]V. N. Belykh, I. V. Belykh, and E. Mosekilde, Phys. Rev. E **63**, 036216 (2001).
[15]A. Yu. Pogromsky and H. Nijmeijer, IEEE Trans. Circuits Syst., I: Fundam. Theory Appl. **48**, 152 (2001).
[16]A. Yu. Pogromsky, G. Santoboni, and H. Nijmeijer, Physica (Amsterdam) **172D**, 65 (2002).
[17]I. Belykh, V. Belykh, K. Nevidin, and M. Hasler, Chaos **13**, 165 (2003).
[18]M. Golubitsky, I. Stewart, and A. Torok, SIAM J. Appl. Dyn. Syst. **4**, 78 (2005).
[19]M. Golubitsky and I. Stewart, Bull. Am. Math. Soc. **43**, 305 (2006).
[20]Y. Wang and M. Golubitsky, Nonlinearity **18**, 631 (2005).
[21]L. M. Pecora, F. Sorrentino, A. M. Hagerstrom, T. E. Murphy, and R. Roy, Nat. Commun. **5**, 4079 (2014).
[22]I. Belykh and M. Hasler, Chaos **21**, 016106 (2011).
[23]H. Kamei and P. J. A. Cock, SIAM J. Appl. Dyn. Syst. **12**, 352 (2013).
[24]Y. Kuramoto, in *International Symposium on Mathematical Problems in Theoretical Physics, Lecture Notes in Physics*, edited by H. Araki (Springer-Verlag, Berlin, 1975), Vol. 39, p. 420.
[25]S. H. Strogatz, Physica (Amsterdam) **143D**, 1 (2000).
[26]A. Pikovsky, M. Rosemblum, and J. Kurths, *Synchronization, a Universal Concept in Nonlinear Sciences* (Cambridge University Press, Cambridge, 2001).
[27]J. A. Acebron, L. L. Bonilla, C. J. Perez Vicente, F. Ritort, and R. Spigler, Rev. Mod. Phys. **77**, 137 (2005).
[28]E. Barreto, B. Hunt, E. Ott, and P. So, Phys. Rev. E **77**, 036107 (2008).
[29]E. Ott and T. M. Antonsen, Chaos **18**, 037113 (2008).
[30]E. A. Martens, E. Barreto, S. H. Strogatz, E. Ott, P. So, and T. M. Antonsen, Phys. Rev. E **79**, 026204 (2009).
[31]H. Hong, H. Chate, H. Park, and L.-H. Tang, Phys. Rev. Lett. **99**, 184101 (2007).
[32]A. Pikovsky and M. Rosenblum, Phys. Rev. Lett. **101**, 264103 (2008).
[33]Yu. Maistrenko, O. Popovych, O. Burylko, and P. A. Tass, Phys. Rev. Lett. **93**, 084102 (2004).
[34]V. Popovych, Y. L. Maistrenko, and P. A. Tass, Phys. Rev. E **71**, 065201 (2005).
[35]V. N. Belykh, V. S. Petrov, and G. Osipov, Regular Chaotic Dyn. **20**, 37 (2015).
[36]Y. Kuramoto and D. Battogtokh, Nonlinear Phenom. Complex Syst. **5**, 380 (2002).
[37]D. M. Abrams and S. H. Strogatz, Phys. Rev. Lett. **93**, 174102 (2004).
[38]D. M. Abrams, R. Mirollo, S. H. Strogatz, and D. A. Wiley, Phys. Rev. Lett. **101**, 084103 (2008).
[39]M. J. Panaggio and D. M. Abrams, Nonlinearity **28**, R67 (2015).
[40]O. E. Omelchenko, Nonlinearity **26**, 2469 (2013).
[41]M. Wolfrum, O. E. Omelchenko, S. Yanchuk, and Yu. L. Maistrenko, Chaos **21**, 013112 (2011).
[42]P. Ashwin and O. Burylko, Chaos **25**, 013106 (2015).
[43]M. J. Panaggio, D. M. Abrams, P. Ashwin, and C. R. Laing, Phys. Rev. E **93**, 012218 (2016).
[44]B. Ermentrout, J. Math. Biol. **29**, 571 (1991).
[45]H.-A. Tanaka, A. J. Lichtenberg, and S. Oishi, Phys. Rev. Lett. **78**, 2104 (1997).
[46]H.-A. Tanaka, A. J. Lichtenberg, and S. Oishi, Physica (Amsterdam) **100D**, 279 (1997).
[47]P. Li, T. K. D. M. Peron, F. A. Rodrigues, and J. Kurths, Sci. Rep. **4**, 4783 (2014).
[48]S. Olmi, A. Navas, S. Boccaletti, and A. Torcini, Phys. Rev. E **90**, 042905 (2014).
[49]S. Olmi, Chaos **25**, 123125 (2015).
[50]M. Komarov, S. Gupta, and A. Pikovsky, Europhys. Lett. **106**, 40003 (2014).
[51]F. Dorfler and F. Bullo, SIAM J. Appl. Dyn. Syst. **10**, 1070 (2011).
[52]Y.-P. Choi, S.-Y. Ha, and S.-B. Yun, Physica (Amsterdam) **240D**, 32 (2011).
[53]S.-Y. Ha, Y. Kim, and Z. Li, SIAM J. Appl. Dyn. Syst. **13**, 466 (2014).
[54]V. N. Belykh, M. I. Bolotov, and G. V. Osipov, Model. Anal. Inf. Syst. **22**, 595 (2015).
[55]A. A. Andronov, A. A. Vitt, and S. E. Khaikin, *Theory of Oscillations* (Pergamon, New York, 1966).
[56]H. Sakaguchi, Phys. Rev. E **73**, 031907 (2006).
[57]F. Tricomi, Ann. Scuola Norm. Sup. Pisa **2**, 1 (1933).
[58]S. H. Strogatz, *Nonlinear Dynamics and Chaos* (Westview Press, Boulder, 2015).
[59]J. Guckenheimer and P. Holmes, *Nonlinear Oscillations, Dynamical Systems, and Bifurcations of Vector Fields*, Applied Mathematical Sciences Vol. 42 (Springer-Verlag, New York, 2002).
[60]V. N. Belykh, N. F. Pedersen, and O. H. Sorensen, Phys. Rev. B **16**, 4853 (1977).
[61]B. P. Demidovich, *Lectures on Stability Theory* (Nauka, Moscow, 1967).